2006

I-V characteristics of Au/Ni Schottky diodes on GaN with SiNx nanonetwork

J. Xie
Virginia Commonwealth University, xiej@vcu.edu

Yi Fu
Virginia Commonwealth University

Xianfeng Ni
Virginia Commonwealth University

S. A. Chevtchenko
Virginia Commonwealth University, chevtchenkos@vcu.edu

Hadis Morkoç
Virginia Commonwealth University, hmorkoc@vcu.edu

Xie, J., Fu, Y., Ni, X., et al. I-V characteristics of Au/Ni Schottky diodes on GaN with SiNx nanonetwork. Applied Physics Letters, 89, 152108 (2006).

I-V characteristics of Au/Ni Schottky diodes on GaN with SiN_x nanonetwork

Jinqiao Xie,[a] Yi Fu, Xianfeng Ni, Serguei Chevtchenko, and Hadis Morkoç
Department of Electrical and Computer Engineering, Virginia Commonwealth University, Richmond, Virginia 23284 and Department of Physics, Virginia Commonwealth University, Richmond, Virginia 23284

(Received 20 July 2006; accepted 24 August 2006; published online 10 October 2006)

Room temperature and temperature dependent current-voltage characteristics of Ni/Au Schottky diodes fabricated on undoped GaN prepared with and without *in situ* SiN_x nanonetwork by metal organic chemical vapor deposition have been studied. The features of the Schottky diodes depend strongly on the SiN_x deposition conditions, namely, its thickness. Reduction in the point and line defect densities caused the Schottky barrier height to increase to 1.13 eV for 5 min SiN_x deposition time as compared to 0.78 eV without SiN_x nanonetwork. Similarly, the breakdown voltage also improved from 76 V for the reference to 250 V when SiN_x nanonetwork was used. With optimized SiN_x nanonetwork, full width at half maximum values of (0002) and $(10\bar{1}2)$ x-ray rocking curves improved to 217 and 211 arc sec, respectively, for a 5.5 μm thick layer, as compared to 252 and 405 arc sec for a reference sample of the same thickness, which are comparable to literature values. The photoluminescence linewidth also reduced to 2.5 meV at 15 K with free excitons A and B clearly resolvable. © *2006 American Institute of Physics*. [DOI: 10.1063/1.2359294]

III-nitride based devices have exhibited phenomenal performance in ultraviolet to visible light-emitting diodes, lasers, ultraviolet detectors, and field effect transistors in past decades.[1] Despite the developments, there is a need to improve the device performance and reliability, particularly in light-emitting diodes for general lighting applications, which in turn require reduction in extended and point defect densities. In this vein, a variety of methods which mainly rely on epitaxial lateral overgrowth[2] (ELO) have been developed. With ELO (Ref. 2) the dislocation density has been reduced to mid-10^6 cm^{-2}. The only disadvantage of ELO is that it requires *ex situ* photolithography and therefore interruption of growth and possible impurity incorporation. Recently, techniques based on microscale ELO using *in situ* deposited SiN_x nanonetwork,[3–7] *ex situ* TiN_x network,[8] and porous SiC (Ref. 9 and 10) have drawn a certain degree of attention. A systematic study of single and double SiN_x nanonetwork schemes has been reported on SiC substrates.[11,12] However, only a cursory optimization of the SiN_x layer was undertaken and the layers were characterized mainly for their structural properties by transmission electron microscopy (TEM) study.[13] In this letter, we report on the effect of SiN_x interlay deposition conditions as it relates to mainly the electrical properties of GaN grown on 2 in. sapphire substrates with mention of the x-ray diffraction data, photoluminescence data, and dislocation density.

GaN epilayers were grown in a vertical low pressure metal organic chemical vapor deposition (MOCVD) system. The structures of the samples investigated in this letter are described in Fig. 1. After a low temperature GaN nucleation layer, ~1 μm GaN was deposited followed by SiN_x deposition without interruption and 4.5 μm undoped GaN film. All samples were unintentionally doped, and the only difference between samples was SiN_x deposition times which varied from 0 (reference), 3, 4, to 5 min. After growth, the surface features of all the samples were investigated using scanning electron microscopy (SEM), and a high resolution x-ray diffraction (XRD) system (X'Pert-MPDTM, Philips) was used to examine the crystalline quality. Schottky diode (SD) current-voltage (*I-V*) and capacitance-voltage (*C-V*) were measured by using Keithly 4200 and HP (Agilent) 4284A.

Planar SDs were fabricated using standard photolithography. Before metallization, all samples were cleaned in acetone, methanol, and de-ionized (DI) water in ultrasonic bath, followed by boiling aqua regia cleaning for 20 and 5 min DI water rinse. Ti/Al/Ti/Au (30/100/30/100 nm) Ohmic contacts were deposited by e-beam and thermal evaporations, followed by a 60 s rapid thermal annealing at 900 °C in nitrogen ambient. Finally, 200 μm diameter Ni/Au (30/120 nm) SDs were deposited by e-beam evaporation. The distance between SDs and Ohmic contacts was 50 μm.

The effect of SiN_x deposition condition on epitaxial structural quality was characterized from the full width at half maximum (FWHM) values of XRD (0002) and $(10\bar{1}2)$ rocking curves. As shown in Fig. 1, the FWHM values of (0002) and $(10\bar{1}2)$ diffractions for 5.5 μm thick GaN with-

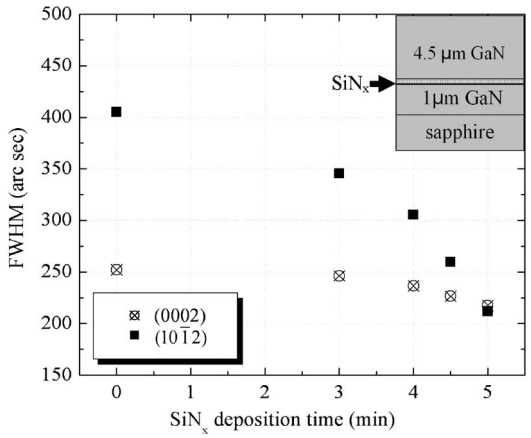

FIG. 1. FWHM values of symmetric (0002) and asymmetric $(10\bar{1}2)$ rocking curve scans for different SiN_x nanonetwork deposition times (0, 3, 4, 4.5, and 5 min). (Scan condition: step size: 0.002°; time/step: 0.4 s; 4×Ge monochromator aperture: 1×1 mm; detector: no slit, and power: 40 kV, 40 mA). (Inset) The schematic sample structure with various SiN_x nanonetwork deposition times.

[a]Electronic mail: xiej@vcu.edu

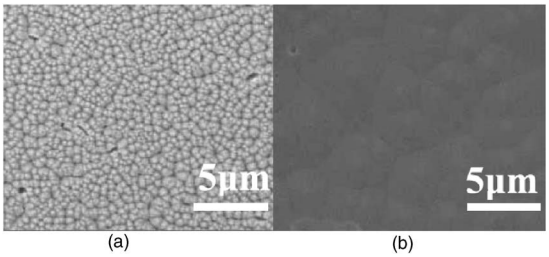

FIG. 2. SEM images reveal the GaN grain size after *in situ* hydrogen annealing at 1000 °C in MOCVD chamber. (a) without SiN_x nanonetwork and (b) with 5 min SiN_x nanonetwork.

out SiN_x nanonetwork are 252 and 405 arc sec, which were comparable to other reports.[14] When the SiN_x nanonetwork was used, the FWHM values were decreased dramatically especially for the asymmetric $(10\bar{1}2)$ diffraction. When the SiN_x deposition time was increased from 3 to 5 min, (0002) and $(10\bar{1}2)$ FWHM values decreased from 246 and 345 arc sec to 217 and 211 arc sec, respectively. Compared to the reference sample, the FWHM value of the $(10\bar{1}2)$ diffraction was reduced nearly by half, indicating a significant improvement of film quality. Since the FWHM values of (0002) and $(10\bar{1}2)$ are correlated to screw-type and edge-type dislocations, respectively, our XRD data suggest that SiN_x nanonetwork can reduce edge-type dislocation density effectively, which is consistent with the earlier study on SiC substrates.[11] The mechanism of dislocation reduction by SiN_x nanonetwork is to reduce the nucleation sites, in other words, grains will be larger. This is confirmed by Fig. 2, which shows SEM surface images of GaN after *in situ* hydrogen etching at 1000 °C in the MOCVD chamber. Using Fig. 2, we get a typical grain size of less than 0.5 μm with a density of 3.2×10^8 cm^{-2} for the reference sample without SiN_x. On the other hand, with 5 min SiN_x deposition, the grain size increases dramatically to over 3 μm with a density of 9.6×10^6 cm^{-2}. Preliminary TEM investigations indicate very effective blocking of edge dislocations by the SiN_x nanonetwork, lowering the density to about 10^7 cm^{-2}. The method was also effective in reducing the screw dislocations whose density stood below mid-10^7 cm^{-2}. From the discussion above, we can conclude that further increases in the SiN_x deposition time will result in more effective dislocation reduction up to a point. However, much thicker GaN over layers or modified growth conditions are needed for coalescence as the SiN_x deposition time deposition time is increased. In our case, when SiN_x deposition time was less than 4.5 min, 3 μm overgrowth is sufficient to achieve smooth surfaces, but 4.5 μm overgrowth is the minimum requirement to get coalesced surfaces for 5 min SiN_x deposition. When SiN_x was deposited for 6 min, we could not get coalesced surface even at 10 μm regrowth under current growth condition employed. The possible reasons are the unoptimized lateral overgrowth rate when islands with $(1\bar{1}01)$ prismatic planes were formed[15] as well as the longer distance between nucleation sites.

Turning our attention to electrical characterization, typical room temperature *I-V* characteristics of Ni/Au SDs are plotted in Fig. 3. As we can see, the saturation current decreases monotonously with increasing SiN_x deposition time from 0 (the control sample) to 5 min, which means that the effective Schottky barrier height increased owing to shallow

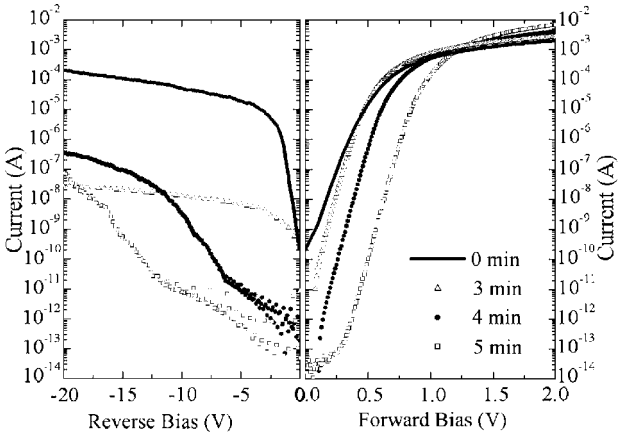

FIG. 3. Room temperature forward and reverse *I-V* characteristics of Ni/Au Schottky diodes with different SiN_x deposition times.

defect reduction. Meanwhile, the series resistance and ideality factor also decreased when longer SiN_x deposition times were used. Based on the thermionic emission model, the forward current density at $V>3(kT/q)$ has the form[1,16]

$$J = J_S[\exp(qV/nkT) - 1], \tag{1}$$

where the saturation current J_s is expressed as

$$J_S = A^{**}T^2 \exp(-q\phi_B/kT), \tag{2}$$

where A^{**} is the effective Richardson constant[1] with a theoretical value of 26.4 $A/cm^2/K^2$, ϕ_B is the barrier height, and n is the ideality factor.

From Eqs. (1) and (2), we calculated the barrier height and ideality factor, which are listed in Table I. For the sample without the SiN_x nanonetwork, the barrier height is 0.76 eV. When the SiN_x deposition time is increased, the barrier height increases from 0.84 eV (3 min SiN_x) to 1.13 eV (5 min SiN_x). At the same time, the ideality factor reduces from 1.3 (no SiN_x) to 1.06 (5 min SiN_x), which indicates that the SDs are nearly ideal in samples grown with the SiN_x nanonetwork. Incidentally, this improved value is consistent with work function of Ni (5.2 eV) and electron affinity of GaN (4.1 eV). In the literature, a value of 1.099 eV (Ni) barrier height was achieved only after GaN surface was treated by $(NH_4)_2S_x$,[17] which is known to passivate the surface defects temporarily. Our results indicated that the Ni Schottky barrier height is very sensitive to the crystalline quality and the excess current is most likely related to the point defects already present in the film, as opposed to being induced during processing as suggested earlier.[18]

The reverse bias *I-V* characteristics are also shown in Fig. 3. It is obvious that when no SiN_x nanonetwork is used, the reverse leakage current is much larger than those in samples with the SiN_x nanonetwork. Consistent with the trend of Schottky barrier height, at low reverse bias

TABLE I. Properties summary of Ni/Au Schottky diodes on GaN with different SiN_x nanonetwork deposition times.

SiN_x (min)	n	$\Phi_{b(I\text{-}V)}$ (eV)	$\Phi_{b(\mathrm{IVT})}$ (eV)	A^* ($A\,cm^{-2}\,K^{-1}$)	Breakdown (V)
0	1.3	0.76	⋯	⋯	76
3	1.13	0.84	0.77	0.0003	250
4	1.08	0.98	0.91	2.07	>210
5	1.06	1.13	1.05	2.66	>210

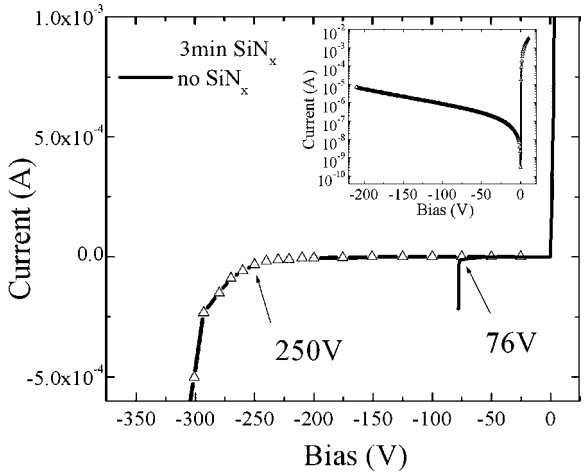

FIG. 4. Reverse breakdown for samples without and with SiN_x nanonetwork. The inset shows a semilog plot of sample with 3 min SiN_x nanonetwork.

(<-10 V) the leakage current decreases when SiN_x deposition time increases. At -10 V, the leakage currents are 1×10^{-11}, 3.3×10^{-9}, and 1.2×10^{-8} A for 5, 4, and 3 min SiN_x nanonetworks, respectively. However, when the reverse bias is higher (>-20 V), the sample with 3 min SiN_x nanonetwork exhibits the lowest leakage current. A more complex current leakage mechanism may play a role here. Nevertheless, it is fair to state that when the SiN_x nanonetwork is used, the leakage current is significantly reduced as compared to the control sample without SiN_x nanonetwork.

To increase our confidence in the Schottky barrier height data, we also performed temperature dependent *I-V* measurements, which led to the activation energy in temperature range of 300–500 K, and results are listed in Table I. The barrier heights calculated from the Richardson plot using Eq. (2) are consistent with the room temperature values for each sample. On the other hand, the calculated effective Richardson constant is much smaller than the theoretically expected value, which is commonly reported in literature.[1] As we can see in Table I, effective Richardson constant is also related to the crystal quality, and obviously further work is required to shed light on the discrepancy between measured and theoretical values endemic to GaN.

To further evaluate the quality of SDs, the reverse breakdown voltages were measured and are shown in Fig. 4. For voltages less than 210 V, we used a Keithly 4200 parameter analyzer. For voltages larger than 210 V, we used a high voltage power supply and continuously increased the bias manually until breakdown. A remarkable improvement of the breakdown was achieved with SiN_x nanonetwork. As can be seen in Fig. 4, the breakdown voltage was -76 V for the reference sample. When 3 min SiN_x nanonetwork was used, it increased to -250 V. This value is comparable to Schottky rectifiers fabricated on bulk[19] and thick hydride vapor phase epitaxy[20] GaN in planar structures without a guard ring or surface passivation. In all the samples with different SiN_x deposition times, the breakdown was observed larger than 210 V, while the 3 min one showed the best uniformity and lowest leakage current at -210 V. This is consistent with the reverse bias *I-V* characteristics, as shown in Fig. 3. Considering the similar background doping, leakage current at high reverse bias seems related to the thickness after coalescence. Since a shorter SiN_x deposition allows coalescence with ease, the top layer after coalescence is much thicker for the 3 min SiN_x deposition than for the 5 min one. However, the real mechanism of leakage current at high reverse bias still needs further investigation.

In summary, the effect of SiN_x nanonetwork deposition conditions, mainly the deposition time, on the electrical properties of AuNi/GaN SDs has been investigated. When 5 min SiN_x nanonetwork was used, nearly ideal SDs were achieved with a barrier height of 1.13 eV and ideality factor of 1.06. Reverse breakdown voltage was also improved to 250 V with SiN_x nanonetwork as compared to 76 V for the control sample. The structural properties of GaN were studied using XRD measurement, and by optimization of SiN_x deposition time, FWHM values of (0002) and $(10\bar{1}2)$ diffractions, as low as 217 and 211 arc sec, were achieved. Consistent with the aforementioned trend is that the photoluminescence line width of the donor bound exciton reduced to 2.5 from 6.7 meV for the control at 15 K, and both free excitons A and B became clearly resolved. Further, the total dislocation density reduced to about mid-10^7 cm^{-2} based on plan view TEM imaging. This work also supports what is already well known in that the crystalline quality strongly affects the Schottky diode characteristics.

The work has been funded by a grant from the Air Force Office of Scientific Research (Kitt Reinhardt). The authors thank T. S. Kuan, W. J. Choyke, R. M. Feenstra, and R. Devaty for discussions and collaborations on the general topic of dislocation reduction in GaN.

[1] H. Morkoç, *Nitride Semiconductors and Devices*, 2nd ed. (Springer, Berlin, to be published), Chap. 5.
[2] P. Gibart, Rep. Prog. Phys. **67**, 667 (2004).
[3] S. Haffouz, H. Lahrèche, P. Vennégues, P. de Mierry, B. Beaumont, F. Omnès, and P. Gibart, Appl. Phys. Lett. **73**, 1278 (1998).
[4] S. Tanaka, M. Takeuchi, and Y. Aoyagi, Jpn. J. Appl. Phys., Part 2 **39**, L831 (2000).
[5] X. L. Fang, Y. Q. Wang, H. Meidia, and S. Mahajan, Appl. Phys. Lett. **84**, 484 (2004).
[6] A. Dadgar, M. Poschenrieder, A. Reiher, J. Blasing, J. Christen, A. Krtschil, T. Finger, T. Hempel, A. Diez, and A. Krost, Appl. Phys. Lett. **82**, 28 (2003).
[7] E. Frayssinet, B. Beaumont, J. P. Faurie, P. Gibart, Zs. Makkai, B. Pécz, P. Lefebvre, and P. Valvin, MRS Internet J. Nitride Semicond. Res. **7**, 8 (2002).
[8] Y. Fu, T. Moon, F. Yun, Ü. Özgür, J. Q. Xie, S. Dogan, H. Morkoç, C. K. Inoki, T. S. Kuan, L. Zhou, and D. J. Smith, Appl. Phys. Lett. **86**, 043108 (2005).
[9] J. Kyeong, H. J. Kim, H. C. Seo, H. J. Kim, E. Yoon, C. S. Hwang, and H. J. Kim, Electrochem. Solid-State Lett. **7**, C43 (2004).
[10] F. Yun, M. A. Reshchikov, L. He, H. Morkoç, C. K. Inoki, and T. S. Kuan, Appl. Phys. Lett. **81**, 4142 (2002).
[11] F. Yun, Y. T. Moon, Y. Fu, K. Zhu, U. Ozgur, H. Morkoç, C. K. Inoki, T. S. Kuan, A. Sagar and R. M. Feenstra, J. Appl. Phys. **98**, 1 (2006).
[12] Ü. Özgür, Y. Fu, Y. T. Moon, F. Yun, H. Morkoç, and H. O. Everitt, J. Appl. Phys. **97**, 103704 (2005).
[13] S. C. Wei, Y. K. Su, S. J. Chang, S.-M. Chen, and W.-L. Li, IEEE Trans. Electron Devices **52**, 1104 (2005).
[14] H. Heinke, V. Kirchner, S. Einfeldt, and D. Hommel, Phys. Status Solidi A **176**, 391 (1999).
[15] K. Hiramatsu, K. Nishiyama, A. Motogaito, H. Miyake, Y. Iyechika, and T. Maeda, Phys. Status Solidi A **176**, 535 (1999).
[16] M. Sze, *Physics of Semiconductor Devices*, 2nd ed. (Wiley, New York, 1981), Chap. 5, p. 258.
[17] C.-T. Lee, Y.-J. Lin, and D.-S. Liu, Appl. Phys. Lett. **79**, 2573 (2001).
[18] H. Hasegawa and S. Oyama, J. Vac. Sci. Technol. B **20**, 1674 (2002).
[19] Y. Zhou, M. Li, D. Wang, C. Ahyi, C.-C. Tin, J. Williams, M. Park, N. M. Williams, and A. Hanser, Appl. Phys. Lett. **88**, 113509 (2006).
[20] Z. Z. Bandic, P. M. Bridger, E. C. Piquette, T. C. McGill, R. P. Vaudo, V. M. Phanse, and J. M. Redwing, Appl. Phys. Lett. **74**, 1266 (1999).